



ELSEVIER

Physics Reports 311 (1999) 451–462

---

---

PHYSICS REPORTS

---

---

# Astrophysical evidence for massive black holes

Ari Laor\*

*Department of Physics, Technion, Haifa 32000, Israel*

---

## Abstract

Massive black holes have long been thought as the most plausible “engine” for bright active galaxies. However, strong independent evidence for the existence of such exotic objects was lacking. This situation has changed dramatically in the past three years with the appearance of new evidence for very massive compact objects in nearby galaxies, and with the possible detection of strong relativistic effects expected near a black hole. Furthermore, it now appears that a massive black hole may exist at the nuclei of most galaxies. Higher quality observations expected in the next few years, may significantly strengthen the case for massive black holes. © 1999 Elsevier Science B.V. All rights reserved.

*PACS:* 98.54.Aj; 97.60.Lf; 98.62.Js; 98.35.Jk

*Keywords:* Quasars; Seyfert galaxies; Black holes

---

## 1. Introduction

This paper describes a somewhat personal view of the recent growth in the astrophysical evidence for massive black holes (MBHs), and no attempt was made to provide complete references. This paper is mainly intended for the general physicist, rather than astrophysicist, as very little a priori knowledge in astrophysics is assumed. Similar recent reviews, with different emphasis, can be found in Rees (1997) and Ho (1998). This paper is organized as follows. A brief description of what are active galaxies, and why they are thought to be powered by MBHs, is described in Section 2. The first independent evidence for MBHs in normal galaxies is briefly described in Section 3, and the recent new evidence based on stellar and gas dynamics is described in Section 4. In Section 5 I describe the new tentative evidence for strong relativistic effects very close to MBHs, and some future prospects are given in Section 6.

---

\* E-mail: laor@physics.technion.ac.il.

## 2. Massive black holes and active galaxies

### 2.1. What are active galaxies?

Quasars were first discovered about 40 years ago. They appeared as point like objects in optical and radio imaging surveys of the sky, and were termed quasi-stellar since their optical fluxes were typical of stars in our Galaxy, i.e. objects with a solar-like luminosity,  $L_{\odot} \sim 4 \times 10^{33} \text{ erg s}^{-1}$ , at distances of a few hundred pc ( $1 \text{ pc} = 3.08 \times 10^{18} \text{ cm}$ ). Schmidt (1963) realized, based on highly red-shifted hydrogen Balmer lines, that these objects are in fact at cosmological distances, i.e. a few hundred Mpc away, and are thus  $10^{12}$  more luminous than previously thought, or 100 times more luminous than a typical bright galaxy. Quasar emission ranges from the radio regime ( $\sim 10^8 \text{ Hz}$ ) to the hard X-ray regime ( $\sim 10^{18} \text{ Hz}$ ), and in some cases up to extremely hard  $\gamma$ -rays at TeV ( $\sim 10^{26} \text{ Hz}$ ). Some quasars show spatially resolved radio emission in the forms of jets, that start at relativistic velocities close to the center, and terminate in giant lobes ( $\sim 10^5 \text{ pc}$  across) as far as a Mpc away. It was later realized that Seyfert galaxies, which show evidence for a non-stellar continuum source at their core, harbor objects similar to quasars, but scaled down in luminosity. Quasars and Seyfert galaxies are grouped together as active galactic nuclei (AGNs), and their luminosity ranges from about  $10^{38}$  to  $10^{48} \text{ erg s}^{-1}$ . A comprehensive discussion of AGNs can be found in Peterson (1997).

### 2.2. Why are massive black holes required?

The typical luminosity of a bright quasar is  $L \sim 10^{46} \text{ erg s}^{-1}$ . Assuming it is not much above the Eddington limit,

$$L_{\text{Edd}} = 1.25 \times 10^{47} M / 10^9 M_{\odot} \text{ erg s}^{-1},$$

implies a minimum binding mass  $M \geq 10^8 M_{\odot}$  ( $M_{\odot} \simeq 2 \times 10^{33} \text{ g}$ ). Optical variability can occur on  $< 100$  days timescale, which implies  $R < 3 \times 10^{17} \text{ cm}$  for the size of the emitting region (e.g. Sirola et al., 1998). X-ray variability can occur on  $< 1$  day timescale (e.g. Mushotzky et al., 1993; Forster and Halpern, 1996), which implies  $R < 3 \times 10^{15} \text{ cm}$ . The gravitational radius, defined as  $R_g \equiv GM/c^2 = 1.5 \times 10^{14} m_{\odot} \text{ cm}$ , where  $M = 10^9 m_{\odot} M_{\odot}$ , is  $> 1.5 \times 10^{13} \text{ cm}$ . The optical emission originates then from  $r < 10^4 R_g$ , and the X-ray emission from  $r < 10^2 R_g$ . Thus, the mass which is required to prevent the quasar from exploding under its own radiation pressure, must be confined to a region not much larger than the black hole event horizon.

One of the defining characteristics of quasars and Seyfert 1 galaxies is broad emission lines having a typical linewidth  $\Delta\lambda/\lambda \sim 0.01$ . The line broadening mechanism cannot be thermal since the gas temperature, as indicated by the ionization state of the elements producing the lines, is  $< 10^5 \text{ K}$ . This temperature corresponds to a thermal broadening of  $\Delta\lambda/\lambda < 2 \times 10^{-4}$ . The most likely line broadening mechanism is highly supersonic bulk motion of gas clouds, requiring typical velocities of  $v \sim 0.01c$ .

The size of this so-called Broad Line Region (BLR) is  $R_{\text{BLR}} = 0.1 L_{46}^{1/2} \text{ pc}$ , where  $L = 10^{46} L_{46} \text{ erg s}^{-1}$  is the bolometric luminosity of the AGN. This size dependence is consistent with ‘‘echo mapping’’ results whereby  $R_{\text{BLR}}$  is measured through the time lag of the emission line

response to changes in the ionizing continuum (Peterson, 1993; Kaspi et al., 1996). This size dependence is also expected based on photoionization models of dusty gas clouds in AGNs (Laor and Draine, 1993; Netzer and Laor, 1993). Gravity most likely dominates the clouds motion. A radial velocity fields is ruled out, suggesting some sort of a virialized velocity field, i.e.  $v^2 \sim GM/r$ , which for  $L_{46} = 1$  and  $v = 0.01c$  gives  $M \sim 10^9 M_\odot$  within  $3 \times 10^{17}$  cm (see Peterson et al., 1998 for specific estimates for some AGNs).

### 2.3. The best guess model

The process which powers quasars is able to generate  $> 10^{13} L_\odot$  from a volume  $< 10^{-9} \text{pc}^3$ . The most plausible mechanism again calls for a MBH, invoking infall of gas, through a thin Keplerian accretion disk, into a MBH (see Rees, 1984 for a review).

This mechanism allows a very high efficiency ( $\epsilon$ ) as 6–30% (for a nonrotating-maximally rotating black hole in a disk) of the accreted rest mass is converted to energy, which implies accretion rates of  $\dot{M} = L/\epsilon c^2 = 1.75 L_{46} (0.1/\epsilon) M_\odot \text{yr}^{-1}$ . Since the potential energy, and for a Keplerian disk, also the dissipated energy, go like  $\sim r^{-1}$  (up to general relativistic correction factors at small  $r$ ), most of the rest mass is converted to energy at a few gravitational radii, i.e.  $r \sim 10^{14}$  cm. Since the disk is thin this energy can be radiated locally, allowing the very high values of  $\Delta L/\Delta t$  observed in AGNs.

Although the acceleration and confinement mechanisms of relativistic jets which are emitted from the cores of some AGNs are not well understood, a MBH may be involved in these processes. These jets appear to have a stable axis over  $> 10^6$  yr, which can be associated with the angular momentum vector of a rotating MBH (Rees, 1984).

An optically thick disk emission is expected to have a peak surface temperature of  $T \sim (L/\pi(3R_g)^2 \sigma_{\text{Boltzman}})^{1/4}$  or  $T \sim 1 - 2 \times 10^5 L_{46}^{1/4} m_9^{-1/2} \text{K}$ , and thus peak emission at  $\lambda \sim 100\text{--}1000 \text{\AA}$  (Shields, 1978), which is generally where the peak  $\nu L_\nu$  of AGNs is indeed observed. The IR emission is well explained by dust reprocessing (e.g. Sanders et al., 1989), and the X-ray power-law emission is most likely associated with Comptonization in hot gas just above the accretion disk (e.g. Mushotzky et al., 1993).

The MBH + accretion disk model thus proved to be a very fruitful paradigm, allowing one to explain most of the observed characteristics of AGNs. This paradigm was formed quite rapidly after the realization that quasars are extremely luminous (Schmidt, 1963; Salpeter, 1964; Zeldovich and Novikov, 1964; Lynden-Bell, 1969), and practically all of the accumulated data over the past 30 years appears to be consistent with it.

But do MBHs actually exist? All the arguments listed above for MBHs in AGNs are rather circumstantial. To answer this question one needs an evidence which is “AGN phenomenology” independent, i.e. one which does not rely on any of the arguments listed above.

## 3. Evidence for compact massive dark objects in normal galaxies

The first independent evidence for the existence of compact massive dark objects, most likely MBHs, was obtained in nearby normal galaxies, where there was no a priori reason to suspect such objects should exist.

The first indication was based on the stellar light distribution very close to the center of giant elliptical galaxies. The observed break in the slope of the stellar power-law light distribution with radius was attributed to the change in the potential produced by a central massive object. The black hole mass is then deduced from the break radius  $r_b$  using the simple relation  $M_{\text{BH}} = r_b \sigma^2 / G$ , where  $\sigma$  is the stellar velocity dispersion outside the black hole radius of influence (e.g. Young et al., 1978). However, this evidence is rather weak as it is generally possible to obtain a break in the stellar light distribution for some (somewhat arbitrary) stellar distribution models without a central massive object.

Stronger cases for MBHs were made based on the detection of a sharp rise in  $\sigma$ , and in some cases also in the ordered rotation velocity, at  $r < r_b$  (e.g. Sargent et al., 1978). The gradual improvement of ground-based telescopes angular resolution over the past few years, allowed stellar velocities to be probed closer to the core, revealing many more nearby galaxies where a MBH is suggested (see Kormendy and Richstone, 1995 for a recent review). However, even for these new MBHs candidates, it is generally possible to fit more complicated stellar velocity fields without the need to invoke a central massive compact dark object.

## 4. New evidence for very compact massive dark objects

### 4.1. On stellar versus gas dynamics

The mean free path to physical stellar collisions is  $l_* = (n_* \times \sigma_*)^{-1}$ , where  $n_*$  is the number density of stars in the Galaxy, and  $\sigma_*$  is the collision cross section. Typically in the Galaxy  $n_* \sim 1 \text{ pc}^{-3}$ , and one can approximate  $\sigma_* \sim (2R_*)^2 \pi$ , i.e. the geometrical collision cross section, where  $R_* \sim 10^{11} \text{ cm}$  is a typical stellar radius (neglecting the ‘‘Coulomb logarithm’’ which corrects for gravitational focusing, but does not affect the final conclusion). We then get  $l_* \sim 10^{32} \text{ cm}$ , which is about  $10^4$  times the radius of the observable universe. Stars therefore form a collisionless system of particles, and there will be a velocity distribution for the stars,  $f_*(\mathbf{v}, \mathbf{r})$ , at each position in space. This complicates the inference of the three-dimensional velocity distribution from the observed line of sight velocity distribution (LOSVD). For example, if stars tend to reside on radial orbits in a spherically symmetric distribution without a central MBH, then the LOSVD would rise sharply towards the center (where the radial orbits parallel our line of sight), mimicking the LOSVD for circular orbits around a central massive object (where the rotation velocity rises towards the center).

On the other hand, for gas particles the collision cross section is  $\sigma_p \sim 10^{-15} \text{ cm}^{-2}$ , and the typical densities in the interstellar medium are  $n_p \sim 1 \text{ cm}^{-3}$ , yielding  $l_p \sim 10^{15} \text{ cm}$ . Thus, the gas can be regarded as a fluid on all scales where its dynamics can be observationally probed. Thus,  $\mathbf{v} = \mathbf{v}(\mathbf{r})$ , i.e. we have just a single valued  $\mathbf{v}$ , rather than  $f_*(\mathbf{v})$ , at each  $\mathbf{r}$ . This simplifies significantly the inference of the three-dimensional particle velocity field from the LOSVD.

The great advantage of stars is their huge surface density,  $M_*/\pi R_*^2 \sim 10^{11} \text{ g cm}^{-2}$ , which implies that only gravity can move stars around. Thus,  $\nabla\phi = -\mathbf{a}$ , i.e. their acceleration provides the gradient in the gravitational potential with essentially no ambiguity. On the other hand, gas particles have  $m_p/\pi r_p^2 \sim 10^{-9} \text{ g cm}^{-2}$ , and so they can be accelerated on short time scales by gas, magnetic, or radiation pressure gradients. Thus, the gas dynamics, as inferred from the line profiles,

may not be related at all to gravity. In addition, the line profile may sometimes not be related at all to the gas dynamics. The energy of a photon is shifted when it is scattered by fast electrons. The typical fractional energy gain per scattering by electrons in a thermal plasma is  $\Delta\varepsilon/\varepsilon = 4kT/m_e c^2 = 7 \times 10^{-4}(T/10^6 \text{ K})$ , and thus broadening due to electron scattering will dominate Doppler broadening produced by bulk motion when  $T/10^6 \text{ K} > v/200 \text{ km s}^{-1}$ .

#### 4.2. *The gas disk in M 87 ( $r \sim 10 \text{ pc}$ )*

The first strong evidence for a massive compact dark object was based on the gas dynamics in the core of the giant elliptical galaxy M 87, as deduced by *HST* imaging and spectroscopy. Ford et al. (1994) discovered a small disk of ionized gas at the center of the galaxy ( $r_{\text{out}} \sim 100 \text{ pc}$ ,  $r_{\text{in}} < 5 \text{ pc}$ ), and Harms et al. (1994) measured the gas velocity at various positions in the disk, revealing it is consistent with a simple Keplerian rotation around a central object with a mass of  $2.4 \pm 0.7 \times 10^9 M_{\odot}$ , within  $\sim 5 \text{ pc}$  from the center, implying a minimum density of  $\sim 10^7 M_{\odot} \text{ pc}^{-3}$ . The amount of starlight within the disk is  $< 10^7 L_{\odot}$ , indicating this central massive object is very dark ( $L/M < 0.01$  solar), and thus cannot be just a very dense cluster of normal stars. However, exotic scenarios invoking a very dense cluster of highly subluminescent stars, such as white dwarfs, neutron stars, or solar mass black holes, cannot be ruled out in this object.

A MBH with practically the same mass was already suspected by Young et al. (1978) based on a break in the stellar light distribution, and by Sargent et al. (1978) based on the rise in stellar velocity dispersion close to the nucleus. The *HST* determination is much more secure since the imaging information provides a nearly unique solution for the orbits of the gas clouds, and the velocity information indicates the gas is affected mostly by gravity (Macchetto et al., 1997 find small deviations from Keplerian orbits). The agreement of the highly simplified analysis of Young et al. and Sargent et al. with the *HST* gas disk results is interesting as it suggests nature may indeed be as simple as these authors assumed.

M 87 also has a large scale jet, and the jet axis is close to parallel to the disk axis. Thus, M 87 appears to follow the “standard AGN paradigm” surprisingly well. It displays an accretion(?) disk, around a MBH, and a jet emanating from the center at right angle to the disk.

#### 4.3. *The water maser in NGC 4258 ( $r \sim 0.1 \text{ pc}$ )*

Some active galaxies produce an intense water maser emission line at 22.2 GHz from their nuclei. This emission line profile typically indicates a large range of velocities for the emitting molecular gas. Since the emission is coherent, a very high surface brightness is achieved by the emitting components which are typically very compact. The very high surface brightness allows one to image these water masers at a very high angular resolution through VLBI interferometric imaging, which go down to  $0''.2$  mas. Miyoshi et al. (1995) and Greenhill et al. (1995) resolved the emission from the core of NGC 4258 with a remarkable spatial resolution of only 0.006 pc. They showed the emitting components are arranged along three linear structures, consistent with a nearly edge on view of warped disk extending from 0.13 to 0.26 pc from the center. In addition, they also obtained the line of sight velocity of each small component, revealing a nearly perfect Keplerian rotation curve in the two outer linear structures.

The deduced dark object mass is  $3.6 \times 10^7 M_\odot$ , implying a density  $> 4 \times 10^9 M_\odot \text{pc}^{-3}$ . The perfect match to a rotation curve around a point-like object rules out any distributed mass within the disk of more than  $4 \times 10^6 M_\odot$ . The disk is extremely thin, with an upper limit of  $H/r < 0.0025$ , indicating  $T < 1000 \text{ K}$  in the disk, as expected for molecular gas. The very small value of  $H/r$  also indicates the lack of any other significant radiation or magnetic forces, which is consistent with the nearly perfect Keplerian rotation curve.

Monitoring of this object over timescales of years revealed the expected velocity drift due to the radial acceleration  $v^2/r$ , and also the expected proper motion on the sky plane, these two effects allow an independent, and highly accurate measurement of the distance of the host galaxy.

#### 4.4. The center of the Milky Way ( $r \sim 0.01 \text{ pc}$ )

The center of our Galaxy is an extremely complex environment, including gas ranging from very cold and molecular ( $T < 100 \text{ K}$ ) to very hot and fully ionized ( $T \sim 10^8 \text{ K}$ ), compact X-ray sources, and a dense cluster of massive young stars. The situation is further complicated by the large extinction along our line of sight which completely obscures the optical and UV emission from this region (see Genzel et al., 1994; Morris and Serabyn, 1996; for recent reviews). Evidence for high stellar velocity dispersions close to the Galactic center, suggesting a  $\sim 10^6 M_\odot$  MBH, accumulated over the past 20 years, but given the complexity of this environment, the case for a MBH remained weak (e.g. Phinney, 1989).

The evidence for a MBH improved dramatically over the past three years following significant improvements in the energy resolution of near IR spectroscopy, and in the spatial resolution of near IR imaging. The new data indicate a rising velocity dispersion towards the center based on the radial velocities (Krabbe et al., 1995), and on the tangential stellar velocities, as measured from the stellar proper motions (Eckart and Genzel, 1996). The combined data sets allow us to deduce the 3-D velocity vector of each star, removing nearly all the ambiguity in the stellar dynamics, and indicates a central mass of  $(2.61 \pm 0.35) \times 10^6 M_\odot$ . The most recent observations (Genzel et al., 1997) reveal several fast moving stars ( $v > 1000 \text{ km s}^{-1}$ ) within 0.01 pc of the Galactic center, indicating a central mass density  $\geq 2.2 \times 10^{12} M_\odot \text{pc}^{-3}$ , which rules out practically all non-black hole models (see also Maoz, 1998).

## 5. New evidence for relativistic effects very close to a black hole ( $r \sim 10^{-3} - 10^{-5} \text{ pc}$ )

### 5.1. Why is the Fe $K\alpha$ line so important?

The strongest line detected in hard X-ray (2–10 keV) spectra of AGNs is the Fe  $K\alpha$  line at 6.4 keV (Pounds et al., 1990). This line is produced by radiative decay of an electron at the 2P level to a vacancy in the ground 1S level. A vacancy at the 1S level can be produced either by collisional ionization or by photoionization which deposit  $> 7.1 \text{ keV}$  in a 1S electron. A significant rate of collisional ionization requires  $T > 10^7 \text{ K}$  (i.e.  $kT > 1 \text{ keV}$ , e.g. Fig. 7 in Sutherland and Dopita, 1993), and at this temperature Fe is more highly ionized than Fe XVII. At such a high ionization state electrons are removed from the  $n = 2$  level, and the  $n = 1$  electrons become more tightly bound to the nucleus since the screening of the nucleus by the  $n = 2$  electron is reduced. Thus, the

$K\alpha$  line energy increases significantly with ionization above Fe XVII, reaching 6.9 keV for H-like Fe (Fe XXVI). Photoionization can occur by an external X-ray continuum source, rather than radiation produced by the gas. Thus, for a dilute enough radiation field, the gas can be rather cold ( $T < 10^4$  K), and the emitted Fe  $K\alpha$  can be at 6.4 keV. The photoionization cross section for the 1S electrons at 7.1 keV is about  $7 \times 10^{-20}$  cm<sup>2</sup>, and given the typical Fe/H abundance ratio of  $\sim 3 \times 10^{-5}$ , one needs a cold gas column  $\geq 10^{24}$  cm<sup>-2</sup> for efficient conversion of the incident X-ray flux to Fe  $K\alpha$  photons.

Thus, the fact that an Fe  $K\alpha$  line at 6.4 keV is common in AGNs provides a clear evidence for X-ray photoionization of cold ( $T < 5 \times 10^6$  K), high column ( $\Sigma > 10^{24}$  cm<sup>-3</sup>) gas.

As mentioned in Section 2.2, the rapid X-ray variability indicates a source size  $< 3 \times 10^{15}$  cm. Since the X-ray continuum also carries a significant fraction of the total AGN flux ( $> 10\%$ ), and the energy production is proportional to  $r^{-1}$ , this continuum source must be located very close to the MBH.

Where is the cold, high column, reprocessing gas located? In some objects where the X-ray emission was monitored (e.g. Iwasawa et al., 1996) there is a rapid response ( $< 1$  day) of the line to continuum variation, indicating the reprocessing gas lies close to the X-ray continuum source. Thin accretion disk models predict the presence of  $T < 5 \times 10^5$  K gas with  $\Sigma > 10^{25}$  cm<sup>-3</sup> down to the innermost stable orbit, and thus the most plausible model for the  $K\alpha$  line is X-ray reprocessing by a thin accretion disk.

## 5.2. The predicted Fe $K\alpha$ line profile

The orbits of particles within a few  $R_g$  of a black hole reach mildly relativistic values ( $\beta \equiv v/c \sim 0.5$ , e.g. Bardeen et al., 1972), and thus one expects significant distortions of the observed line profile due to both Doppler broadening and gravitational redshifts.

If the accretion disk is indeed thin (as suggested by the low gas temperature indicated by a 6.4 keV  $K\alpha$  line), then the gas orbits are most likely close to Keplerian. One can then obtain for a given black hole spin parameter ( $a$ ), a unique and accurate solution for the predicted line profile as a function of radius and inclination of the orbit, with no free parameters. The predicted line profile from the whole disk is, however, a function of the line surface emissivity  $j(r)$ , which is not known a priori since there is no complete theory for the spatial distribution of the ionizing X-ray continuum.

The observed line profile results from the combination of two effects: (1) Doppler shift and Doppler beaming, (2) gravitational redshift. The first effect produces a double-peaked line from each radius, with a blue peak which is always stronger than the red peak. At small distances the red peak is strongly suppressed and the line appears like a highly skewed, single peaked, line (e.g. Fig. 1 in Laor, 1991). The second effect just shifts the whole line to the red.

Fig. 1 shows the predicted line profile for a range of possible  $j(r)$  from a disk around a maximally rotating black hole in a disk ( $a = 0.9982$ , Thorne, 1974). Although the details of the line profiles are strongly dependent on the specific  $j(r)$ , in all cases one gets a significantly broadened line ( $\Delta\varepsilon/\varepsilon \sim 0.1$ – $0.5$ ) with a steep blue wing and a much more extended red wing. The line peak is generally blueshifted, unless the disk is observed with  $\cos\theta > 0.9$ , where  $\theta$  is the angle between the disk axis and the line of sight. These characteristics serve as the “signature” of a line produced in a disk close to a black hole.

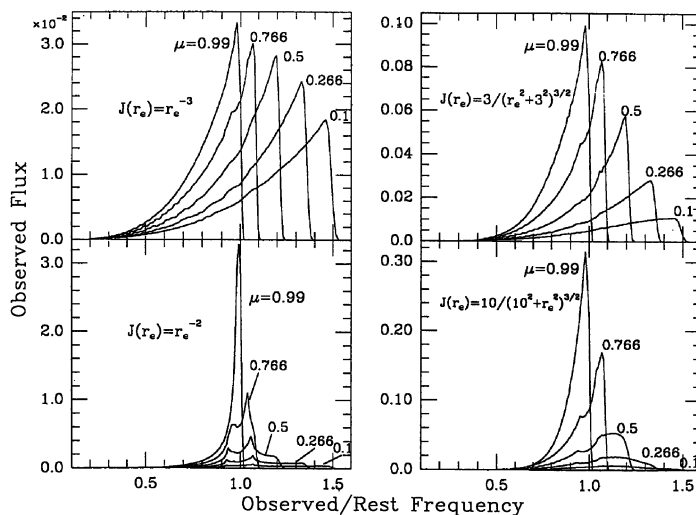


Fig. 1. Line profiles for various emissivity laws for a disk around a rotating black hole (Laor, 1991). The emissivity law and the observed inclination ( $\mu = \cos \theta$ ) are marked in each panel.

If the black hole is non-rotating ( $a = 0$ ), then the marginally stable orbit (i.e. inner disk radius), is at  $6R_g$ , rather than  $1.23R_g$  (Page and Thorne, 1974) and the relativistic effects on the line profile are somewhat less extreme (Fabian et al., 1989). Fig. 2 shows the contribution to the line profile from the innermost disk at  $r < 6R_g$ , which ranges from a highly blueshifted strong peak for a nearly edge on disk, to a weak highly-reddened component for a nearly face on disk. Thus, very high S/N observations of the  $K\alpha$  line profile may allow us to constrain both  $j(r)$  and the black holes spin (see also Reynolds and Begelman, 1997).

### 5.3. The observed Fe $K\alpha$ line profile

*GINGA* was the first satellite to reveal the presence of the Fe  $K\alpha$  in AGNs, but its low energy resolution ( $\Delta\varepsilon/\varepsilon \sim 0.17$  at 6.4 keV) and generally low S/N spectra did not allow one to resolve the line profile. The next Japanese satellite in this series *ASCA*, which is still active, has about 10 times higher energy resolution and it was able to resolve this line for the first time in AGNs (see Fig. 3). In the few objects where a reasonable S/N was obtained the line profile appears to be remarkably similar to the thin disk prediction, having in practically all cases a steep blue wing and an extended red wing (e.g. Tanaka et al., 1995; Mushotzky et al., 1995). Analysis of about 20 Seyfert galaxies by Nandra et al. (1997) allows one to deduce the distribution of disk inclinations. It indicates that almost all AGNs are observed at  $1 \geq \cos \theta \geq 0.5$ . This distribution is remarkably similar to the one expected based on AGN unification schemes (e.g. Antonucci, 1993; Urry and Padovani, 1995), which assume a thick torus co-planar with the accretion disk, which obscures the continuum source and the BLR at  $\cos \theta < 0.5$ .

Fabian et al. (1995) explored whether the observed asymmetric and highly broadened  $K\alpha$  profile can be produced by other physical mechanisms, specifically Comptonization in cold gas,

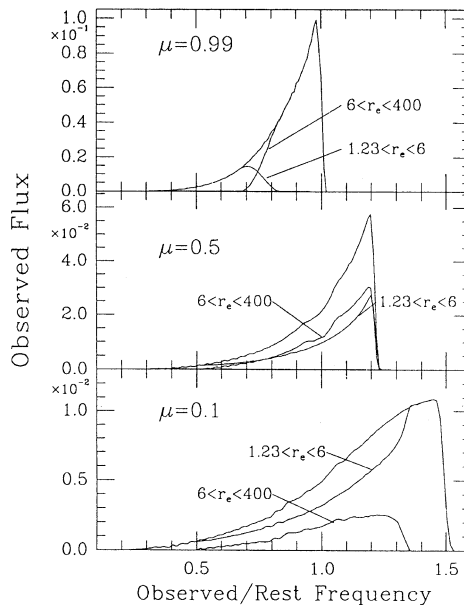


Fig. 2. Decomposition of the line according to the emission region, as marked in each panel. The outer disk ( $6R_g < r < 400R_g$ ) approximates a disk around a nonrotating black hole.

or an outflow, and concluded that these mechanisms cannot naturally explain the observed profiles.

## 6. Future prospects

Significant advances in the quality of the evidence for MBHs is expected in the near future along various lines.

Images of nearby ellipticals with the *HST* indicates that nuclear gas disks/rings are rather common (Ford et al., 1997). Spectroscopic mapping of the velocity field of some of these objects, however, indicate deviations from Keplerian rotation which are more significant than in M 87, and thus the evidence for a central massive object is less robust in these objects (Ferrarese et al., 1996; Bower et al., 1998; van der Marel and van den Bosch, 1998). Additional spectroscopic observations, in particular of very thin gas disks, in non active galaxies (so that radiation pressure is not likely to be significant), and in galaxies with very massive black holes ( $> 10^9 M_\odot$ ), at small distances from the core (so that the MBH gravity dominates), may yield additional strong cases like the one in M 87. Accumulating a significant number of MBH candidates would allow one to study the distribution function of MBH, and their relation to the host galaxy properties.

The discovery of the nearly perfect Keplerian water maser disk in NGC 4258 prompted extensive searches for more similar objects (Braatz et al., 1996). However, the few more water maser disks discovered are significantly thicker and show non-Keplerian dynamics, indicating significant

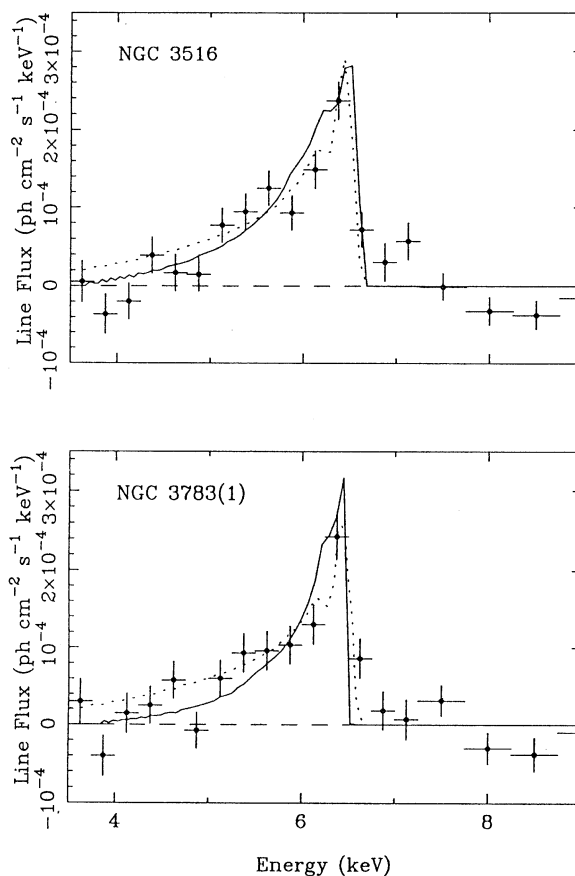


Fig. 3. Observed line profiles for NGC 3516 and NGC 3227 with *ASCA* (Nandra et al., 1997). The best-fit nonrotating (solid line) and rotating (dotted line) black hole models are also shown.

pressure gradients are present (Greenhill et al., 1996, 1997). Apparently, the very favorable conditions in NGC 4258, i.e. an extremely thin disk ( $h/r < 0.0025$ ), indicating lack of any significant non gravitational forces, and the very close to edge on view (required for a significant maser amplification), are rare. It is thus not likely that a significant number of additional such objects will be discovered.

Significant advances are expected in the X-ray front in the near future with the launch of the European satellite *XMM* and the Japanese satellite *ASTRO-E* in the years 1999 and 2000. These X-ray telescopes will have a 10–100 times higher energy resolution, and significantly larger collecting areas, which will allow a very significant improvement in the measured Fe  $K\alpha$  line profile. The improved line profile will allow us to establish whether the disk interpretation is correct, and together with monitoring of X-ray continuum and line variability it may allow us to deduce the geometry and the dynamics of the accretion flow very close to the event horizon of MBHs.

One of the most dramatic recent results from *HST* is the suggestion by Magorrian et al. (1998) that practically all galaxies may have a MBH at their core, and that the black hole mass is

correlated with the mass of the bulge (see also Kormendy and Richstone, 1995). These results were derived from ground based spectroscopy together with high angular resolution *HST* imaging of the stellar light distribution close to the core. This claim is still somewhat controversial since the observed rise in the velocity dispersion may still be explained by anisotropic stellar velocity distribution models in most of their objects. However, spectroscopic observations which are being conducted now with *HST* will test if the velocity dispersion continues to rise towards the center, as expected for MBHs, and may thus make the case for MBHs significantly more robust. If the Magorrian et al. suggestion is verified then MBHs are not just exotic objects found in the small fraction of galaxies which are active, but are just as common as galaxies are, and may be an inevitable outcome of galaxy formation.

The existence of MBHs may soon become a closed issue. However, theoretical questions such as how were MBHs formed? how are they fueled? and how do they produce relativistic jets? are likely to remain open for many more years.

## References

- Antonucci, R., 1993. *Annu. Rev. Astron. Astrophys.* 31, 473.
- Bardeen, J.M., Press, W.H., Teukolsky, S.A., 1972. *Astrophys. J.* 178, 347.
- Bower, G.A. et al., 1998. *Astrophys. J.* 492, L111.
- Braatz, J.A., Wilson, A.S., Henkel, C., 1996. *Astrophys. J. Suppl.* 106, 51.
- Eckart, A., Genzel, R., 1996. *Nature* 383, 415.
- Fabian, A.C., Rees, M.J., Stella, L., White, N.E., 1989. *Mon. Not. R. Astron. Soc.* 242, 14.
- Fabian, A.C. et al., 1995. *Mon. Not. R. Astron. Soc.* 277, L11.
- Ferrarese, L., Ford, H.C., Jaffe, W., 1996. *Astrophys. J.* 470, 444.
- Ford, H.C. et al., 1997. In: Wickramasinghe, D.T., Bicknell, G.V., Ferrario, L. (Eds.), *Accretion Phenomena and Related Outflows*, IAU Colloquium 163. ASP Conference Series.
- Forster, K., Halpern, J.P., 1996. *Astrophys. J.* 468, 565.
- Genzel, R., Eckart, A., Ott, T., Eisenhauer, F., 1997. *Mon. Not. R. Astron. Soc.* 291, 219.
- Genzel, R., Hollenbach, D., Towns, C.H., 1994. *Rep. Prog. Phys.* 57, 417.
- Greenhill, L.J., Jiang, D.R., Moran, J.M., Reid, M.J., Lo, K.Y., Claussen, M.J., 1995. *Astrophys. J.* 440, 619.
- Greenhill, L.J., Gwinn, C.R., Antonucci, R., Barvainis, R., 1996. *Astrophys. J.* 472, L21.
- Greenhill, L.J., Moran, J.M., Herrnstein, J.R., 1997. *Astrophys. J.* 481, L23.
- Greenhill, L.J., Herrnstein, J.R., Moran, J.M., Menten, K.M., Velusamy, T., 1997. *Astrophys. J.* 486, L15.
- Ho, L.C., 1998. In: Chakrabarti, S.K. (Ed.), *Observational Evidence for Black Holes in the Universe*. Kluwer, Dordrecht, in press (astro-ph/9803307).
- Iwasawa, K. et al., 1996. *Mon. Not. R. Astron. Soc.* 282, 1038.
- Kaspi, S., Smith, P.S., Maoz, D., Netzer, H., Jannuzi, B.T., 1996. *Astrophys. J.* 471, L75.
- Kormendy, J., Richstone, D.O., 1995. *Annu. Rev. Astron. Astrophys.* 33, 581.
- Krabbe, A. et al., 1995. *Astrophys. J.* 447, L95.
- Laor, A., 1991. *Astrophys. J.* 376, 90.
- Laor, A., Draine, B.T., 1993. *Astrophys. J.* 402, 441.
- Lynden-Bell, D., 1969. *Nature* 223, 690.
- Magorrian et al., 1998. *Astron. J.* 115, 2285.
- Maoz, E., 1998. *Astrophys. J.* 494, L181.
- Miyoshi, M., Moran, J., Herrnstein, J., Nakai, N., Diamond, P., Inoue, M., 1995. *Nature* 373, 127.
- Morris, M., Serabyn, E., 1996. *Annu. Rev. Astron. Astrophys.* 34, 645.
- Mushotzky, R.F., Done, C., Pounds, K.A., 1993. *Annu. Rev. Astron. Astrophys.* 31, 717.

- Mushotzky, R.F., Fabian, A.C., Iwasawa, K., Matsuoka, M., Nandra, K., Tanaka, Y., 1995. *Mon. Not. R. Astron. Soc.* 272, L9.
- Nandra, K., George, I.M., Mushotzky, R.F., Turner, T.J., Yaqoob, T., 1997. *Astrophys. J.* 477, 602.
- Netzer, H., Laor, A., 1993. *Astrophys. J.* 404, L51.
- Page, D.N., Thorne, K.S., 1974. *Astrophys. J.* 191, 499.
- Peterson, B.M., 1993. *PASP* 105, 247.
- Peterson, B.M., 1997. *An Introduction to Active Galactic Nuclei*. CUP, Cambridge.
- Peterson, B.M. et al., 1998. *Astrophys. J.* in press (astro-ph/9802104).
- Phinney, E.S., 1989. In: Moris, M. (Ed.), *IAU Symp. 136, The Center of the Galaxy*. Kluwer, Dordrecht, p. 543.
- Pounds, K.A., Nandra, K., Stewart, G.C., George, I.M., Fabian, A.C., 1990. *Nature* 344, 132.
- Rees, M.J., 1984. *Annu. Rev. Astron. Astrophys.* 22, 471.
- Rees, M.J., 1997. In: Wald, R. (Ed.), *Black Holes and Relativity*. Chandrasekhar Memorial Conf. (astro-ph/9701161), in press.
- Reynolds, C.S., Begelman, M.C., 1997. *Astrophys. J.* 488, 109.
- Salpeter, E.E., 1964. *Astrophys. J.* 140, 796.
- Sanders, D.B., Phinney, E.S., Neugebauer, G., Soifer, B.T., Mathews, K., 1989. *Astrophys. J.* 347, 29.
- Sargent, W.L.W., Young, P.J., Boksenberg, A., Shortridge, K., Lynds, C.R., Hartwick, F.D.A., 1978. *Astrophys. J.* 221, 731.
- Schmidt, M., 1963. *Nature* 197, 1040.
- Shields, G.A., 1978. *Nature* 272, 706.
- Sirola, C.J. et al., 1998. *Astrophys. J.* 495, 659.
- Sutherland, R.S., Dopita, M.A., 1993. *Astrophys. J. Suppl.* 88, 253.
- Tanaka, Y. et al., 1995. *Nature* 375, 659.
- Thorne, K.S., 1974. *Astrophys. J.* 191, 507.
- Urry, C.M., Padovani, P., 1995. *PASP* 107, 803.
- van der Marel, R.P., van den Bosch, F.C., 1998. *Astron. J.* submitted (astro-ph/9804194).
- Young, P.J., Westphal, J.A., Kristian, J., Wilson, C.P., Landauer, F.P., 1978. *Astrophys. J.* 221, 721.
- Zeldovich, Ya.B., Novikov, I.D., 1964. *Sov. Phys. Dokl.* 158, 811.